1

Background and Essentials

1.1 Introduction

Radiation physics is the science of ionizing radiation and its interaction with matter, with special interest in the energy absorbed. Radiation dosimetry deals with the quantitative determination of that energy. This introductory chapter lays the ground for the different types of ionizing radiation sources that will be covered in this book and the overall classification of the mechanisms of energy transfer to matter, emphasizing its stochastic nature. The concept of interaction cross section and mean free path (MFP), of importance for the treatment of charged and uncharged particle interactions in the following chapters, is included in this chapter along with a description of the most common kinematic relativistic expressions. The interaction of radiation with matter leads to the ionization and excitation of the atom and, as a result, vacancies are created in the atomic shells and the atom is left in an excited state; the excited ion then relaxes to its ground state through radiative and non-radiative transitions. The process of atomic relaxation occurs during both charged and uncharged particle interactions with matter (even when only excitation occurs) and is also included in this chapter. The final section deals with the evaluation of uncertainties applicable to many of the chapters that follow, describing dosimetry detectors, measurements, and calculations.

1.2 Types and Sources of Ionizing Radiation

Ionizing radiation is generally characterized by its ability to excite and ionize atoms of matter with which it interacts. Since the energy needed to cause a valence electron to escape an atom is of the order of 4 eV–25 eV, radiation must carry kinetic or quantum energies in excess of this magnitude in order to be called 'ionizing'. As will be seen from Eq. (1.1), this criterion would seem to include electromagnetic radiation with wavelengths up to about 320 nm, which includes most of the ultraviolet (UV) radiation band (~10 nm–400 nm). However, for practical purposes, these marginally ionizing UV radiations are not usually considered in the context of radiation physics and dosimetry, as they

Fundamentals of Ionizing Radiation Dosimetry, First Edition. Pedro Andreo, David T. Burns, Alan E. Nahum, Jan Seuntjens, and Frank H. Attix.

are even less capable of penetrating through matter than is visible light, while other ionizing radiations are generally more penetrating. The physics of the interaction of optical lasers and radiofrequency (RF) sources of electromagnetic radiation with matter is very different from that for ionizing radiation, and is not covered in this book.

The following types of ionizing radiation will be considered:

(a) Charged particles
  (i) *Electrons*: These are light charged particles, and when their charge is positive they are called *positrons*. If they are emitted by a radionuclide they are usually referred to as β rays (positive or negative). If they result from a charged-particle collision they are referred to as 'knock-on' electrons (KOe) or 'delta rays' (δ). Intense, continuous beams of electrons up to 25 MeV are available from Van de Graaff generators, and pulsed electron beams of much higher energies are available from linear accelerators ('linacs'), betatrons, and microtrons. Descriptions of such accelerators, mostly addressed to radiation medicine applications, have been given, for example, by Karzmark *et al.* (1993) and Podgorsak (2010).
  (ii) *Heavy charged particles*: These are nuclei of atoms with some or all of the atomic electrons removed; ions of nuclei with an atomic number equal to, or smaller than, that of neon nuclei ($Z = 10$) are referred to as *light ions*. Heavy charged particles usually obtain their kinetic energy from acceleration by a Coulomb force field in a Van de Graaff, cyclotron, synchrotron, or heavy-particle linear accelerator. Alpha particles are also emitted by some radionuclides. The various types include the following:
    – Proton – the hydrogen nucleus
    – Deuteron – the deuterium nucleus, consisting of a proton and neutron bound together by the nuclear force
    – Triton – a proton and two neutrons similarly bound
    – α-particle – the helium nucleus, that is, two protons and two neutrons. ^{3}He particles have one less neutron.
    – Other heavy charged particles consisting of the nuclei of heavier atoms, either fully stripped of electrons or having a different number of electrons than necessary to produce a neutral atom.

  A recommendation for using the term *protons and heavier charged particles* has been issued jointly by the ICRU and the IAEA (Wambersie *et al.*, 2004). Some relevant properties of light and heavy charged particles are given in Appendix A.

(b) Uncharged particles
  (i) γ *rays*: These are electromagnetic radiation emitted from a nucleus or in annihilation reactions between positrons and electrons. The energy of a photon is given by

$$k = h\nu = \frac{hc}{\lambda} = \frac{1.2398 \text{ keV nm}}{\lambda \text{ nm}} \tag{1.1}$$

  where h is Planck's constant (4.136×10^{-18} keV s, with 1 keV $= 1.6022 \times 10^{-16}$ J) and c is the velocity of light *in vacuo* (2.998×10^8 m s^{-1}). The momentum of a photon is given by $p = k/c$.

Evidently, from Eq. (1.1), the energy of a photon of 0.1 nm wavelength is 12.4 keV. The range of photon energies emitted by radioactive atoms extends from 2.6 keV (K-edge characteristic x rays from electron capture in $^{37}_{18}$Ar) to the 6.1 MeV and 7.1 MeV γ rays from $^{16}_{7}$N.

(ii) *x rays*: These are electromagnetic radiation emitted by charged particles (usually electrons) in changing atomic energy levels (called *characteristic* or *fluorescence* x rays, see Section 1.6) or in slowing down in a Coulomb force field (*continuous* or *bremsstrahlung* x rays, see Chapter 2). Note that x-ray and γ-ray photons of a given energy are particles with identical properties, differing only in their origin. The energy ranges of x rays, referred to by the voltage used to accelerate electrons that produce bremsstrahlung photons, are commonly known as

0.1–20 kV	Low-energy, 'soft' x rays, or 'Grenz rays'
20–120 kV	Diagnostic-range x rays
120–300 kV	Orthovoltage x rays
300 kV–1 MV	Intermediate-energy x rays
1 MV upward	Megavoltage x rays

(iii) *Neutrons*: These are neutral particles obtained from nuclear reactions (e.g., (p, n) or fission), as they cannot themselves be accelerated electrostatically.

The range of energies most frequently used in applications of ionizing radiation extends from 10 keV to 25 MeV for electrons and photons, neutrons up to 100 MeV, protons up to 300 MeV, and heavier charged particles up to 400 MeV/m_u, where m_u is the atomic mass unit (also denoted by 'u', see Appendix A) . Electrons and photons down to about 1 keV are also of interest in a number of applications, and so are energies up to about 50 MeV.

Traditionally, the terminology used for ionizing radiation emphasizing key differences between the interactions of charged and uncharged particles with matter has been *directly ionizing radiation* and *indirectly ionizing radiation*. This classification was prone to misunderstanding because all particles of a given energy excite or ionize matter *directly*, and it is the energy transferred to the target medium that can be direct or indirect. Thus, the classification of particles used throughout this book is in terms of energy transfer:

(a) *Direct energy transfer*: Charged particles, which deliver their energy to matter directly through multiple small Coulomb-force interactions along the particle tracks.

(b) *Indirect energy transfer*: Uncharged particles, that is, x- or γ-ray photons or neutrons, which first transfer their energy to charged particles in the matter through which they pass, in relatively few 'major' interactions. The resulting fast charged particles in turn deliver the energy to matter as in (a). The transfer and deposition of energy in matter by photons and neutrons is therefore a *two-step process*.

The reason that so much attention is paid to ionizing radiation and that a whole science dealing with these radiations and their interactions with matter has evolved stems from the unique effects that such interactions have upon the irradiated material. Biological systems (e.g., humans) are particularly susceptible to damage by ionizing radiation, so that the expenditure of a relatively trivial amount of energy ($\sim$4 J kg^{-1}) throughout the body is likely to cause death, even though that amount of energy can only raise the gross temperature by about 0.001 °C. Clearly, the ability of ionizing radiation to impart energy to individual atoms, molecules, and biological cells has a profound effect on the outcome. The resulting high local concentrations of absorbed energy can 'kill' a cell either directly or indirectly through the formation of highly reactive chemical species such as free radicals[1] in water, which constitutes the bulk of the biological material. Ionizing radiation can also produce gross changes, either desirable or undesirable, in organic compounds by breaking molecular bonds or, in crystalline materials, by causing defects in the lattice structure. Even structural steel will be damaged by large enough numbers of fast neutrons, becoming brittle and more likely to fracture under mechanical stress.

Discussing the details of such radiation effects, however, lies beyond the scope of this book. Here, we will concentrate on the basic physics of the interactions and methods for measuring and describing the energy absorbed in terms that are useful in the various applications of ionizing radiation.

1.3 Consequences of the Random Nature of Radiation

Suppose we consider a point P in a field of ionizing radiation, and ask, "How many particles will strike P per unit time?" The answer is of course zero, as a point has no cross-sectional area with which the particles can collide. Therefore, the first step in describing the radiation field at P is to associate some non-zero or finite volume with the point. The simplest such volume would be a sphere centered at P, which has the advantage of presenting the same cross-sectional target area to radiation incident from all directions. The next question is how large this imaginary sphere should be. That depends on whether the physical quantities we wish to define with respect to the radiation field are *stochastic* or *non-stochastic*.

A stochastic quantity has the following characteristics:

(a) Its values occur randomly and hence cannot be predicted. However, the probability of any particular value is determined by a probability distribution.
(b) It is defined for finite (i.e., non-infinitesimal) domains only. Its values vary discontinuously in space and time, and it is meaningless to speak of its gradient or rate of change.
(c) In principle, its separate values can each be measured with an arbitrarily small error.

1 A free radical is an atom or compound in which there is an unpaired electron, such as H or CH_3, see Chapter 13.

(d) The *expectation value* $E[x]$ of a stochastic quantity x is the mean of its measured values, $\overline{x}$, as the number n of observations approaches ∞. That is, $\overline{x} \to E[x]$ as $n \to \infty$.

A non-stochastic quantity, on the other hand, has the following characteristics:

(a) For given conditions, its value can, in principle, be predicted by calculation.
(b) It is, in general, a 'point function' defined in an infinitesimal volume; hence it is a continuous and differentiable function of space and time, and one may speak of its spatial gradient and time rate of change. In accordance with common usage in physics, the argument of a legitimate differential quotient may always be assumed to be a non-stochastic quantity.
(c) Its value is equal to, or based on, the *expectation value* of a related stochastic quantity, if one exists. Although non-stochastic quantities in general need not be related to stochastic quantities, they are so related in the context of ionizing radiation.

It can be seen from these considerations that the volume of the imaginary sphere surrounding the point P may be small but must be *finite* if we are dealing with stochastic quantities. It may be infinitesimal ($\mathrm{d}\mathcal{V}$) with reference to non-stochastic quantities. Likewise, the cross-sectional area ($\mathrm{d}a$) and mass ($\mathrm{d}m$) of the sphere, as well as the irradiation time ($\mathrm{d}t$), may be expressed as infinitesimals in dealing with non-stochastic quantities. Since the most common and useful quantities describing ionizing radiation fields and their interactions with matter are all non-stochastic, we defer further discussion of stochastic and non-stochastic dosimetric quantities until Chapter 4.

In general, one can assume that a 'constant' radiation field is strictly random with respect to how many particles arrive at a given point per unit area and time interval. It can be shown that the number of particles observed in repetitions of measurements (assuming a fixed detection efficiency and time interval, and no systematic change of the field vs time) will follow a Poisson distribution. For large numbers of events, this may be approximated by the normal (Gaussian) distribution. If $E[x]$ is the expectation value of the number of particles detected per measurement, the standard deviation of a single random measurement x relative to $E[x]$ is equal to

$$s(x) = \sqrt{E[x]} \approx \sqrt{\overline{x}} \tag{1.2}$$

and the corresponding percentage standard deviation is

$$s(x)_{\%} = \frac{100\ s(x)}{E[x]} = \frac{100}{\sqrt{E[x]}} \approx \frac{100}{\sqrt{\overline{x}}} \tag{1.3}$$

that is, a single measurement would have a 68.3% chance of lying within $\pm s(x)$ of the expectation value $E[x]$, where $s(x)$ is given by Eq. (1.2) if the fluctuations are due to the stochastic nature of the field itself. Further, x would have a 95.5% chance of lying within $\pm 2\ s(x)$ of $E[x]$ or a 99.7% chance of lying within $\pm 3\ s(x)$.

The approximation of $E[x]$ by the mean value $\overline{x}$ in Eqs. (1.2) and (1.3) is necessary because $E[x]$ is unknown but can be approached as closely as desired by the mean value $\overline{x}$ of N measurements, that is, $\overline{x} \to E[x]$ as $N \to \infty$. It is useful to know

how closely $\bar{x}$ is likely to approximate $E[x]$ for a given number of measurements N. This information is conveyed by the standard deviation of the mean value $\bar{x}$ relative to $E[x]$

$$s(\bar{x}) = \frac{s(x)}{\sqrt{N}} = \sqrt{\frac{E[x]}{N}} \approx \sqrt{\frac{\bar{x}}{N}} \tag{1.4}$$

and the corresponding percentage standard deviation is

$$s(\bar{x})_{\%} = \frac{100\ s(\bar{x})}{E[x]} = \frac{100}{\sqrt{N\ E[x]}} \approx \frac{100}{\sqrt{N\ \bar{x}}} = \frac{100}{\sqrt{x_{\text{tot}}}} \tag{1.5}$$

where $x_{\text{tot}} = N\ \bar{x}$ is the total number of particles detected in all N measurements combined. $\bar{x}$ will have a 68.3% chance of lying within $\pm s(\bar{x})$ of $E[x]$. Note that in Eq. (1.5) it makes no difference how many measurements (N) are made in acquiring a given total count x_{tot}, and thus a given value of $s(\bar{x})_{\%}$.

It is important to emphasize that the foregoing statements of standard deviation in Eqs. (1.2)–(1.5) are based exclusively upon the stochastic nature of radiation fields, not taking account of instrumental or other experimental fluctuations. Thus, one should expect to observe experimentally greater standard deviations than these, but never smaller values. This leads us to concepts of accuracy and uncertainty, which are discussed in Section 1.7.

1.4 Interaction Cross Sections

Experimentally determined or calculated results of the interaction of particles with matter are usually expressed in terms of characteristic quantities called *cross sections*. Following a definition given by Joachain (1975), "the cross section of a certain type of event in a given interaction is the ratio of the number of events of this type per unit time and per unit of target particle, to the relative number of the incident particles with respect to the target."

Let us first consider the general case of two particle types, S and T, both having well-defined quantum states. A very narrow parallel monoenergetic beam consisting of $\dot{N}_{\text{in}}$ particles of type S impinges per unit time and per unit area (perpendicular to the direction of the incident beam)[2] on a target made of particles of type T. The direction of incidence is the z-axis (see Figure 1.1) and the target is assumed to be very thin and to contain n_{T} particles in the narrow area covered by the incident beam. It is also assumed that the incident particles S do not interact with each other.

Let $\dot{N}_{\text{out}}$ denote the total number of particles S that have interacted per unit time with the n_{T} target particles and that are scattered in a given direction, where they are measured with a detector. Under the experimental conditions schematized in Figure 1.1, it is obvious that the total number of particles $\dot{N}_{\text{out}}$ is directly

2 This quantity will be defined in Chapter 4 as the *fluence rate*, following ICRU Report 85a (ICRU, 2011) on *Fundamental Quantities and Units for Ionizing Radiation*. In the literature it is often called *current* or *flux*.

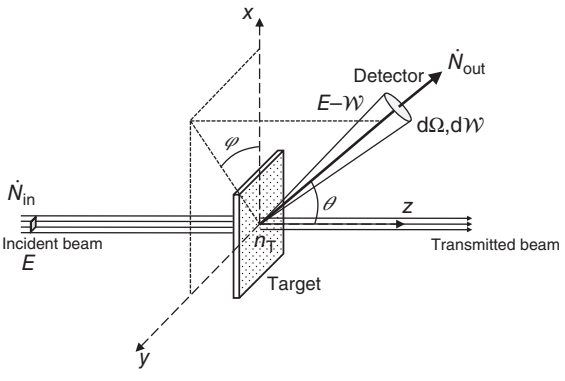

Figure 1.1 Illustration of the quantities used in the definition of interaction cross sections.

proportional to the relative number of incident particles $\dot{N}_{in}$ and to the number n_T of target particles, that is,

$$\dot{N}_{out} \propto \dot{N}_{in}\, n_T = \sigma_{tot}\, \dot{N}_{in}\, n_T \tag{1.6}$$

from where

$$\sigma_{tot} = \frac{\dot{N}_{out}}{\dot{N}_{in}\, n_T} \tag{1.7}$$

where the proportionality factor σ_{tot} has the dimension of area (as the quantity $\dot{N}_{in}$ is per unit area). The quantity σ_{tot} is called the *total cross section* (TCS) for the interaction of particles S with the target particles T and can be considered as the *effective area* that the incident beam 'sees' of the target. Considering only one target particle ($n_T = 1$), we can define $\sigma_{tot} = \dot{N}_{out}/\dot{N}_{in}$ (consistent with the definition above) as the total probability for an incident particle to interact with one target particle and therefore be removed from the incident beam.

We can now introduce the concept of *differential cross section* (DCS), where, rather than counting all scattered particles, we take their energy and direction into consideration. Hence, we assume that the incident particles of energy E lose a certain energy $\mathcal{W}$ and are deflected in a specific direction. This type of interaction mechanism occurs, for example, in the inelastic collisions of charged particles (Chapter 2) or in the Compton scattering of photons (Chapter 3). The detector will record particles that have lost an energy between $\mathcal{W}$ and $\mathcal{W} + \mathrm{d}\mathcal{W}$ and are deflected within a small solid angle $\mathrm{d}\Omega$ in the direction (θ, φ), where θ and φ are the polar and azimuthal angles, respectively.

If we denote by $\dot{N}_{\mathrm{d}\Omega,\mathrm{d}\mathcal{W}}$ the number of detected particles, we can write, as in Eq. (1.6) and considering $n_T = 1$,

$$\dot{N}_{\mathrm{d}\Omega\mathrm{d}\mathcal{W}} \propto \dot{N}_{in}\, \mathrm{d}\Omega\, \mathrm{d}\mathcal{W} \Rightarrow \dot{N}_{\mathrm{d}\Omega\mathrm{d}\mathcal{W}} = \frac{\mathrm{d}^2\sigma}{\mathrm{d}\Omega\, \mathrm{d}\mathcal{W}}\, \dot{N}_{in}\, \mathrm{d}\Omega\, \mathrm{d}\mathcal{W} \tag{1.8}$$

where the proportionality factor

$$\frac{\mathrm{d}^2\sigma}{\mathrm{d}\Omega\, \mathrm{d}\mathcal{W}} = \frac{\dot{N}_{\mathrm{d}\Omega,\mathrm{d}\mathcal{W}}}{\dot{N}_{in}\, \mathrm{d}\Omega\, \mathrm{d}\mathcal{W}} \tag{1.9}$$

is termed the *double-differential cross section* (DDCS) per unit solid angle and per unit energy loss. The DDCS has dimensions of [area solid-angle^{-1} energy^{-1}]

and the product $(\mathrm{d}^2\sigma/(\mathrm{d}\Omega\ \mathrm{d}\mathcal{W})) \times \mathrm{d}\Omega\ \mathrm{d}\mathcal{W}$ represents the area perpendicular to the direction of the incident beam reached by scattered particles within a solid angle $\mathrm{d}\Omega(\theta, \varphi)$ with energies between $E - \mathcal{W} - \mathrm{d}\mathcal{W}$ and $E - \mathcal{W}$.

Integrating the DDCS over solid angle we get the DCS differential in energy loss,

$$\frac{\mathrm{d}\sigma}{\mathrm{d}\mathcal{W}} = \int \frac{\mathrm{d}^2\sigma}{\mathrm{d}\Omega\ \mathrm{d}\mathcal{W}}\ \mathrm{d}\Omega \tag{1.10}$$

and a similar integration of the DDCS over the energy loss $\mathcal{W}$ yields the DCS differential in solid angle,

$$\frac{\mathrm{d}\sigma}{\mathrm{d}\Omega} = \int_0^E \frac{\mathrm{d}^2\sigma}{\mathrm{d}\Omega\ \mathrm{d}\mathcal{W}}\ \mathrm{d}\mathcal{W} \tag{1.11}$$

Integrating any of these DCS, for example, Eq. (1.10) over energy losses, we obtain the TCS as

$$\sigma_{\mathrm{tot}} = \int_0^E \frac{\mathrm{d}\sigma}{\mathrm{d}\mathcal{W}}\ \mathrm{d}\mathcal{W} = \int_0^E \left(\int_\Omega \frac{\mathrm{d}^2\sigma}{\mathrm{d}\Omega\ \mathrm{d}\mathcal{W}}\ \mathrm{d}\Omega \right) \mathrm{d}\mathcal{W} \tag{1.12}$$

The quantum mechanical description of a process, say interaction without energy loss (i.e., elastic scattering), assumes an incident plane wave characterized by the wave function $\psi_{\mathrm{in}} = e^{ikz}$ and corresponding to a particle of mass m with momentum $\mathbf{p} = \hbar\,\mathbf{k}$ and energy $E = p^2/2m = (\hbar k)^2/2m$ and, after interacting with the target, the radially-scattered wave is characterized by $\psi_{\mathrm{out}} = f(\theta, \varphi)\ e^{ikr}/r$, where $f(\theta, \varphi)$ is the so-called *scattering amplitude* (note that quantities in bold characters correspond to vectors). Assuming azimuthal symmetry, $f(\theta, \varphi)$ can be replaced by $f(\theta)$. Taking into account the definition of particle current density (which approximately corresponds to the $\dot{N}_{\mathrm{in}}$ above) in terms of the incident wave ψ_{in} and its conjugate ψ^*_{in}, it can be demonstrated (see, e.g., Liboff, 1992) that

$$\frac{\mathrm{d}\sigma}{\mathrm{d}\Omega} = |f(\theta)|^2 \tag{1.13}$$

that is, the DCS is given by the square of the scattering amplitude.

The TCS of a particle at a given energy is obtained by adding up the cross sections of the various possible interactions in a medium. This is usually expressed in cm^2 or in barns ($10^{-24}\ \mathrm{cm}^2$) per atom or per electron, and is referred to as the *microscopic* total cross section, for example,

$$\sigma_{\mathrm{tot}}(E) = \sum_{i=1}^{n} \sigma_{\mathrm{i}}(E) \tag{1.14}$$

where the various $\sigma_{\mathrm{i}}(E)$ are the cross sections for interactions of the type elastic, ionization, excitation, bremsstrahlung, nuclear, etc, which will be discussed in the following chapters.

When the number of atoms per mass of an element, $N_{\mathrm{a}} = N_{\mathrm{A}}/A$, is taken into account, the total cross section is expressed as

$$\Sigma_{\mathrm{tot}}(E) = \sigma_{\mathrm{tot}}(E)\ \frac{N_{\mathrm{A}}}{A} \tag{1.15}$$

and is termed the *macroscopic* total cross section, typically in $\mathrm{cm^2\ g^{-1}}$ or $\mathrm{m^2\ kg^{-1}}$, where N_A is the Avogadro constant and A is the atomic mass number of the element.

Similarly, the number of electrons per unit mass is given by $N_\mathrm{e} = Z\,N_\mathrm{a} = Z\,N_\mathrm{A}/A$, where Z is the atomic number. The atomic density and electron density, that is, their number per unit volume $\mathcal{V}$, are given by $n_\mathrm{a} = N_\mathrm{a}/\mathcal{V} = \rho N_\mathrm{A}/A$ and $n_\mathrm{e} = Z n_\mathrm{a} = \rho Z N_\mathrm{A}/A$, respectively, where ρ is the mass density ($\mathrm{g\ cm^{-3}}$). Recall that $Z/A \in [0.4, 0.5]$ for all elements except hydrogen, for which $Z/A \approx 1$.[3]

The so-called *mass attenuation coefficient*, $\mu(E)/\rho$, typically in $\mathrm{cm^2\ g^{-1}}$ (or in $\mathrm{m^2\ kg^{-1}}$), is the macroscopic equivalent of the total cross section, that is, $\mu(E)/\rho \equiv \Sigma_\mathrm{tot}(E)$. When multiplied by the mass density it yields the *linear attenuation coefficient*, $\mu(E)$, in $\mathrm{cm^{-1}}$ (or in $\mathrm{m^{-1}}$). In either case, the probability that an interaction will occur in a small distance Δs is given by $\mu \Delta s$.

The mean free path (MFP), which is defined as the inverse of the total macroscopic cross section, or of the relevant attenuation coefficient, yields the mean path length between two consecutive interactions

$$\mathrm{MFP}(E) = \frac{A}{\rho\, N_\mathrm{A} \sigma_\mathrm{tot}(E)} = \frac{1}{\mu(E)} \tag{1.16}$$

It is emphasized that the concept of MFP(E) applies to *all kinds of particles*, charged and uncharged, even if traditionally it is applied more commonly to uncharged particles, such as photons or neutrons. We will return to this concept in the following chapters.

1.5 Kinematic Relativistic Expressions

Some useful relativistic kinematic relationships, used mainly in the chapters dealing with the interaction of charged and uncharged particles with matter (Chapters 2 and 3, respectively), are presented in this section where, with a few exceptions, relativistic expressions can be related to the more familiar classical ones. The equations below avoid differences between large quantities that can arise in relativistic calculations, and their relativistic and non-relativistic limits are straightforward.

The relativistic mass of a particle m with velocity v is related to its rest mass m_0 at $v = 0$ through

$$m = \frac{m_0}{\sqrt{1 - \left(\frac{v}{c}\right)^2}} = \frac{m_0}{\sqrt{1 - \beta^2}} \tag{1.17}$$

where $\beta = v/c$ and c is the speed of light in vacuum. These two fundamental relations yield the following expressions for the particle kinetic energy E and its

3 In neutron physics it is common to define the macroscopic cross section in terms of the atomic density, n_a, that is, $\Sigma_\mathrm{tot}(E) = \sigma_\mathrm{tot}(E)\ n_\mathrm{a}$, which yields units of $\mathrm{cm^{-1}}$ (or $\mathrm{m^{-1}}$).

momentum p:

$$E = \frac{m\ v^2}{2} = \frac{m_0 c^2 \beta^2}{2\ \sqrt{1-\beta^2}}$$
$$p = m\ v = \sqrt{2\ m\ E} = \frac{m_0 c\ \beta}{\sqrt{1-\beta^2}} \tag{1.18}$$

Note that the momentum of a particle is commonly expressed in units of $p\ c$, which has dimensions of energy (e.g., MeV); thus,

$$p\ c = \frac{m_0 c^2\ \beta}{\sqrt{1-\beta^2}} \tag{1.19}$$

Other useful expressions can be derived by squaring Eq. (1.17), which, on rearranging terms, yields

$$m^2 \left(1 - \frac{v^2}{c^2}\right) = m_0^2$$
$$(mc)^2 - m_0^2 c^2 = (mv)^2 \equiv p^2 \tag{1.20}$$

and multiplying both sides by c^2 results in

$$(p\ c)^2 = (mc^2)^2 - (m_0 c^2)^2 \tag{1.21}$$

where mc^2 can be identified with the total energy of the particle, E_{tot}, that is, the well-known Einstein equation $E_{\text{tot}} = mc^2$, and $m_0 c^2$ is the particle rest energy. Equation (1.21) is commonly illustrated as the triangular mnemonic rule shown in Figure 1.2, which includes the well-known relation

$$E_{\text{tot}} = E + m_0 c^2 \tag{1.22}$$

between the total and kinetic energy of a particle through its rest energy.

The combination of Eqs. (1.21) and (1.22) provides useful relations between kinetic energy and momentum in the form

$$p\ c = \sqrt{E(E + 2\ m_0 c^2)} = E\ \sqrt{1 + \frac{2\ m_0 c^2}{E}} \tag{1.23}$$

$$E = \sqrt{(p\ c)^2 + (m_0 c^2)^2} - m_0 c^2 \tag{1.24}$$

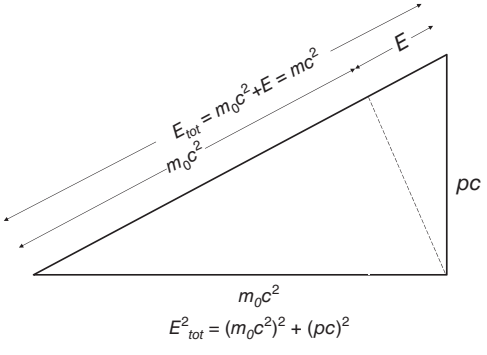

Figure 1.2 Triangular mnemonic rule relating the total energy, E_{tot}, rest energy, $m_0 c^2$, and momentum (in units of $p\ c$) of a particle.

These expressions show that for particles with zero rest mass (photons, neutrinos), $m_0 = 0$, and the momentum is given by $p = E/c$. Similarly, from Eq. (1.22), their relativistic mass is $m = E/c^2$. Their relativistic velocity is

$$\beta = \frac{v}{c} = \frac{p}{m\,c} = 1 \tag{1.25}$$

that is, $v = c$ for $m_0 = 0$.

Note that the right-hand side of Eq. (1.23) includes the inverse of the ratio between the kinetic energy and the rest energy of a charged particle, a ratio frequently denoted by $\tau = E/m_0c^2$, which describes the kinetic energy of a charged particle in units of its rest energy. This is often used to express the relativistic velocity β as

$$\beta^2 = \frac{\tau(\tau + 2)}{(\tau + 1)^2} \tag{1.26}$$

whereas a useful expression as a function of the kinetic energy is

$$\beta^2 = \frac{E(E + 2\ m_0c^2)}{(E + m_0c^2)^2} \tag{1.27}$$

Some expressions in Chapters 2 and 3, dealing with the interactions of charged and uncharged particles with matter, respectively, are often written in terms of the *Lorentz relativistic factor*, γ, defined as

$$\gamma = \frac{1}{\sqrt{1 - \beta^2}} = \tau + 1 \tag{1.28}$$

which yields the simplified expressions for the total and kinetic energy of a particle:

$$\begin{aligned} E_{\text{tot}} &= \gamma\ m_0c^2 \\ E &= (\gamma - 1)\ m_0c^2 \end{aligned} \tag{1.29}$$

However, to avoid confusion with the γ symbol used in other areas of radiation physics and dosimetry, its use will be minimized in this book.

1.6 Atomic Relaxations

As a result of the interactions by charged and uncharged particles in the field of an atomic electron, and of certain radionuclide disintegrations, leading to the ionization of an atom, vacancies are created in the atomic shells and the atom is left in an excited state. Processes that create vacancies are inelastic collisions of charged particles and electron impact ionization (see Chapter 2), photon–atom (photoelectric and Compton) and positron annihilation following a pair production (Chapter 3), and electron capture and internal conversion (Chapter 18). Depending on the nature and energy of the interaction, as well as on the atomic number of the target atom, the vacancy may occur in the outer shell or in one of the inner shells of the atom. The excited ion then 'relaxes' to its ground state. Typically, the excitation energy is released through the transition of

an electron from a higher atomic shell to fill the shell vacancy. The difference in binding energies between the initial and final shell or subshell is emitted through a sequence of *radiative* and *non-radiative* transitions. In radiative transitions, photons (fluorescent x rays) are emitted, and in non-radiative transitions Auger, Coster–Kronig, or super Coster–Kronig electrons are emitted.

The energy of the emitted particles resulting from the relaxation process is determined by the energy levels of the shells or subshells involved in the transition. These transitions are governed by quantum mechanical selection rules that apply to the quantum numbers of the shells and subshells. The quantum numbers involved are

(a) the *principal quantum number n* with values $n = 0, 1, 2, 3, \ldots$;
(b) the *orbital angular momentum quantum number* ℓ with values $\ell = 0, 1, 2, \ldots, n-1$, which corresponds to the electron orbital angular momentum $L = \hbar\sqrt{\ell(\ell+1)}$;
(c) the *magnetic quantum number* m_ℓ determining the z-component of the angular momentum, $L_z = m_\ell \hbar$, with $m_\ell = -\ell, -\ell+1, \ldots, \ell-1, \ell$;
(d) the *intrinsic angular momentum* or *spin quantum number* s with value $s = 1/2$, which corresponds to the spin $S = \hbar\sqrt{s(s+1)} = \hbar\sqrt{3}/2$, and the quantum number m_s, which determines the z-component of the intrinsic angular momentum, $S_z = m_s\hbar$, with $m_s = -1/2, +1/2$.

If there is no interaction between the orbital and the spin angular momenta, the state of atomic electrons is determined by the four quantum numbers, n, ℓ, m_ℓ, and m_s. In reality, there is a coupling between the orbital and the spin angular momenta, leading to the quantum state for the coupled vector $\mathbf{J} = \mathbf{L} + \mathbf{S}$ determined by the quantum numbers j and m_j. The vector $\mathbf{J}$ can take the values $J = \hbar\sqrt{j(j+1)}$ with $j = |\ell - s|, |\ell - s + 1|, \ldots, |\ell + s|$ (with $s = 1/2$) and $m_j = -j, -j+1, \ldots, +j$ determining the z-component of the coupled state $J_z = \hbar\, m_j$. With *spin–orbit coupling*, the state of the electrons is thus determined by the four quantum numbers, n, ℓ, j, m_j.

Transition selection rules for the so-called normal x-ray lines, based on the electric dipole selection rules, dictate the main allowed transitions according to

$$\Delta\ell = +1, -1 \quad \text{and} \quad \Delta j = 0, +1, -1$$

Magnetic dipole and electric quadrupole selection rules give rise to other transitions, but the intensity of these transitions is significantly weaker than those resulting from the electric dipole selection rules. The correspondence between the quantum numbers (n, ℓ, j), with $j = \ell \pm 1/2$, and the various atomic electron subshells, as well as the so-called *shell occupation number* (maximum number of electrons in a subshell, given by $2j + 1$) is given in Table 1.1.

In the fields of photoelectron spectroscopy (XPS), Auger electron spectroscopy (AES), and electron probe microanalysis (EPMA), the current trend for the notation of transitions is that of the International Union of Pure and Applied Chemistry (IUPAC, cf. Jenkins *et al.*, 1991), where the codes of the shells with the initial and final vacancies are written explicitly, separated by a hyphen, for example, K–L2 and K–L1–L2 for radiative and non-radiative transitions, respectively. This

Table 1.1 Correspondence between the quantum numbers ($n\ \ell\ j$), where $j = \ell \pm 1/2$, and the atomic electron subshells, denoted by their spectroscopic or x-ray-level notation.

n	ℓ	j	f_i	Shell notation	
				Spectroscopic	x-ray level
1	0	1/2	2	$1s_{1/2}$	K
2	0	1/2	2	$2s_{1/2}$	L1
2	1	1/2	2	$2p_{1/2}$	L2
2	1	3/2	4	$2p_{3/2}$	L3
3	0	1/2	2	$3s_{1/2}$	M1
3	1	1/2	2	$3p_{1/2}$	M2
3	1	3/2	4	$3p_{3/2}$	M3
3	2	3/2	4	$3d_{3/2}$	M4
3	2	5/2	6	$3d_{5/2}$	M5
4	0	1/2	2	$4s_{1/2}$	N1
4	1	1/2	2	$4p_{1/2}$	N2
4	1	3/2	4	$4p_{3/2}$	N3
4	2	3/2	4	$4d_{3/2}$	N4
4	2	5/2	6	$4d_{5/2}$	N5
4	3	5/2	6	$4f_{5/2}$	N6
4	3	7/2	8	$4f_{7/2}$	N7

The parameter f_i is the *shell occupation number* (maximum number of electrons in a subshell), given by $2j + 1$.

has superseded Siegbahn's notation (developed only for radiative transitions), where the designation of x-ray lines is by the letter code of the shell that had the initial vacancy followed by a Greek letter and, in some cases, a numeral subscript and superscript, for example, $K\beta_4^{II}$ (for K–N4). The correspondence between the two notations is given in Table 1.2.

The energy released through the emission of photons or electrons depends on the energy of the shell or subshell involved, and thus on the atomic number Z. Vacancies created by charged-particle inelastic collisions and Compton scattering of photons occur mostly in outer shells, as the cross section for the creation of inner-shell vacancies through these processes is lower (see Section 3.6.3 regarding the effect of binding on Compton electrons). In contrast, the probability for inner-shell vacancies through photoelectric interactions of photons increases with increasing shell ionization energy, and hence with atomic number. Figure 1.3 shows the shell binding energies U_B for the K, L, M, and N shells and subshells as a function of atomic number Z; numerical values are given in Appendix A.

1.6.1 Radiative and Non-radiative Transitions

As mentioned above, the ionization of an atom produces a vacancy in the atomic subshell $Si(n_i\ \ell_i\ j_i)$ with $i = 0, 1, 2$, etc, from which the electron was ejected. This

Table 1.2 Radiative transitions for the relevant groups in the K, L, and M series.

Group	Lines		Group	Lines	
Kα	K–L2	(Kα_2)		L2–N6	(Lυ)
	K–L3	(Kα_1)		L2–N7	(Lυ)
Kβ	K–M2	(Kβ_3)		L2–O1	(Lγ_8)
	K–M3	(Kβ_1)		L2–O4	(L γ_6)
	K–M4	(Kβ_5^{II})	L_3 ℓ	L3–M1	(Lℓ)
	K–M5	(Kβ_5^{I})	L_3 t	L3–M2	(Lt)
	K–N2	(Kβ_2^{II})	L_3 s	L3–M3	(Ls)
	K–N3	(Kβ_2^{I})	L_3 α	L3–M4	(Lα_2)
	K–N4	(Kβ_4^{II})		L3–M5	(Lα_1)
	K–N5	(Kβ_4^{I})	L_3 β	L3–N1	(Lβ_6)
$L_1\beta$	L1–M2	(Lβ_4)		L3–N4	(Lβ_{15})
	L1–M3	(Lβ_3)		L3–N5	(Lβ_2)
	L1–M4	(Lβ_{10})	L_3 u	L3–N6	(Lu)
	L1–M5	(Lβ_9)		L3–N7	(Lu)
$L_1\gamma$	L1–N2	(Lγ_2)	Mγ	M2–N5	(Mγ)
	L1–N3	(Lγ_3)	Mβ	M4–N6	(Mβ)
	L1–N4	(Lγ_1)	Mξ	M5–N2	(Mξ_2)
$L_2\eta$	L2–M1	(Lη)		M5–N3	(Mξ_1)
$L_2\beta$	L2–M3	(Lβ_{17})	Mα	M5–N6	(Mα_2)
	L2–M4	(Lβ_1)		M5–N7	(Mα_1)
$L_2\gamma$	L2–N1	(Lγ_5)			
	L2–N4	(Lγ_1)			

Transitions for the indicated lines are represented using the IUPAC notation (S0–S1) and the corresponding Siegbahn notation is indicated in parentheses.
Source: Llovet *et al.* (2014). Reproduced with permission of American Institute of Physics.

vacancy is filled by an electron from a higher subshell 'jumping down,' initiating a cascade of radiative and non-radiative transitions as the vacancy migrates to outer subshells and the atom relaxes back to the stable configuration:

(a) In a radiative S0–S1 transition ($n_0 \leq n_1$), a vacancy in subshell S0 is filled by an electron from an outer subshell S1 (the vacancy moves from S0 to S1) and a photon is emitted with an energy k equal to the energy difference of the two shells, that is,

$$k = U_{\mathrm{S0}} - U_{\mathrm{S1}} \tag{1.30}$$

where U_{Si} denotes the binding energy of the Si subshell. These photons are called *characteristic x rays*, as their energy is characteristic of the energy levels of the atomic subshells. The emission process is called *fluorescence*.

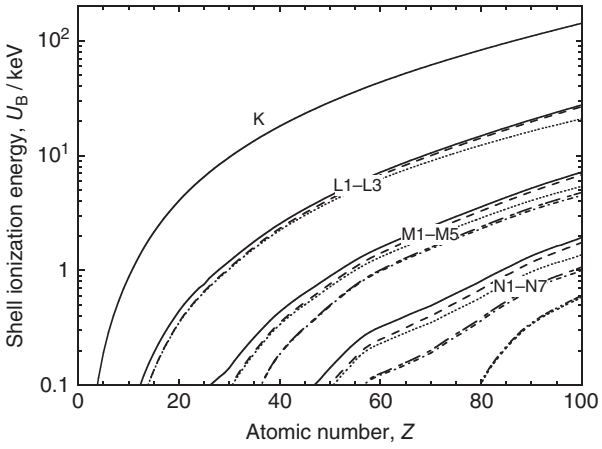

Figure 1.3 Shell binding energies for the K-, L-, M-, and N-shells as a function of atomic number (see Appendix A). (Data from Carlsson, 1975.)

(b) In a non-radiative S0–S1–S2 transition, the vacancy in subshell S0 is filled by an electron from a higher subshell S1 and an electron is ejected from a subshell S2 with an energy

$$E = U_{S0} - (U_{S1} + U_{S2}) \tag{1.31}$$

The subshell from where the electron is ejected can be the same as the one where the vacancy was created (but a different shell), or one further out. The process thus results in an additional vacancy in the ion, that is, two electron vacancies are produced in these transitions. Depending on the subshells involved in non-radiative emissions, these are classified into *Auger*, *Coster–Kronig*, and *Super Coster–Kronig* transitions as follows (see Figure 1.4):

- If the subshells S1 and S2 are in shells different from S0 (where the initial vacancy was created), the process is called an *Auger transition*; this is therefore an *inter-shell* transition.
- If S0 and S1 are in the same shell, the process is called a *Coster–Kronig Transition*; this is an *intra-shell* transition.
- If the three subshells involved S0, S1, and S2 are in the same shell, the process is called a *Super Coster–Kronig transition*; this is also an *intra-shell* transition.

Non-radiative transitions are mostly responsible for the relaxation of vacancies in the L-subshells and above, but Auger transitions are the only alternative to fluorescence produced by K-shell vacancies. When energetically allowed, Coster–Kronig and Super Coster–Kronig transitions dominate over the Auger effect, and multiply further the number of vacancies. Figure 1.4 illustrates the three types of transitions (using the IUPAC notation), which are often referred to with the global name of *Auger transitions*. From a dosimetry point of view, both radiative and non-radiative emissions have particular importance. If emission of fluorescence x rays occurs, energy is transported away from the interaction

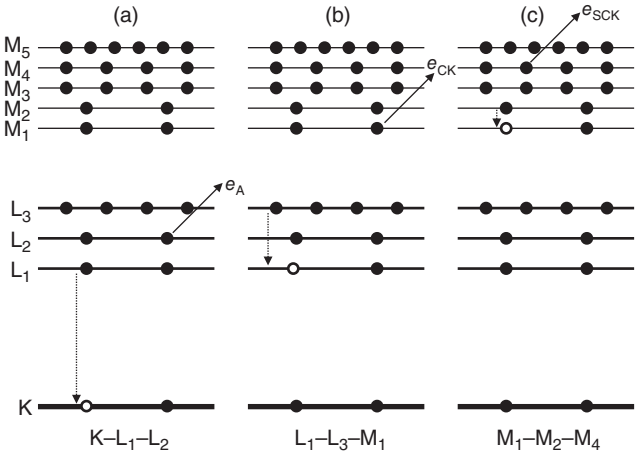

Figure 1.4 Schematic illustration of the non-radiative transitions Auger (a), Coster–Kronig (b), and Super Coster–Kronig (c). In an Auger transition, an electron e_A is ejected from a higher shell; the transition shown is K–L_1–L_2. In a Coster–Kronig transition, a vacancy in any subshell is filled by an electron in a higher subshell in the same shell, with the ejection of an electron e_{CK} from a higher shell (L_1–L_3–M_1 shown). In a Super Coster–Kronig transition, the electron e_{SCK} is ejected from the same shell (M_1–M_2–M_4 shown).

site that would otherwise be deposited locally (other phenomena, such as their contribution to x-ray spectra, are also of importance, see Chapter 7). Auger transitions, on the other hand, deposit energy practically 'on the spot' as the electrons produced have very low energy and therefore the distance they can travel is negligible; furthermore, as their average energy deposition per distance travelled (the stopping power, see Chapter 2) is quite high, the radiobiological effect that they produce is also relatively high. These aspects have favored the use of radionuclides disintegrating via electron capture and/or internal conversion for nuclear medicine therapy applications, termed *targeted Auger-electron therapy* (cf. AAPM, 1993, 1995).

1.6.2 Transition Probabilities and Fluorescence and Auger Yields

The probability for an x-ray emission from a given shell, versus that for the emission of an Auger electron, both being competing mechanisms, is described by the respective *emission yields* of the shell. In general, radiative transitions are more probable for elements of high Z (>30), whereas non-radiative transitions are more probable for low-Z elements (<30). Following the descriptions by Perkins *et al.* (1991a) and Llovet *et al.* (2014), for example, these probabilities are derived in terms of the width of the transitions, often using data derived by Scofield (1969, 1973, 1974).

Let τ_{S0} be the mean lifetime of the excited state of an atom having a vacancy in the subshell S0; the inverse of τ_{S0} is the probability per unit time of a transition to a lower-energy state. The width of the energy level of the initial excited state is, by virtue of the uncertainty principle, $\Gamma_{S0} = \hbar/\tau_{S0}$, and is given by the addition of the partial widths of all the radiative and non-radiative transitions, Γ_{S0-S1} and

$\Gamma_{S0-S1-S2}$, respectively, that fill a vacancy in the subshell S0. The quantity

$$P_{S0-S1} = \frac{\Gamma_{S0-S1}}{\Gamma_{S0}} \tag{1.32}$$

describes the probability that the vacancy in subshell S0 is filled through the radiative transition S0–S1. Likewise, the probability that the vacancy is filled through the non-radiative transition S0–S1–S2 is

$$P_{S0-S1-S2} = \frac{\Gamma_{S0-S1-S2}}{\Gamma_{S0}} \tag{1.33}$$

and both satisfy the condition

$$\sum_{S1} P_{S0-S1} + \sum_{S1,S2} P_{S0-S1-S2} \equiv 1 \tag{1.34}$$

where the summations are over all subshells S1 and S2 with binding energies less than U_{S0}.

The LLNL Evaluated Atomic Data Library (EADL, Perkins *et al.*, 1991a) is the most comprehensive and widespread database of transition probabilities available. It contains data for isolated neutral atoms of the elements $Z = 1 - 100$ with a single vacancy in all the subshells of the K-, L-, M-, N-shells and some O-subshells. Both radiative and non-radiative emissions include transition probabilities as well as the level widths, calculated with an electron-independent model using a Dirac–Hartree–Fock–Slater potential adjusted to reproduce the Z-dependence of the fluorescence yields (see below). For a heavy element, the number of transitions involved in the cascade back to neutrality can be very large. For example, in the case of uranium with an initial vacancy in the K-shell, over 1000 non-radiative transitions and close to 100 radiative transitions are possible. A very large population of such atoms would exhibit a spectrum with many lines; however, the average number of transitions a single such atom would actually experience is much fewer, just over 10 non-radiative and about 8 radiative transitions. A computer code named *RELAX* written by Cullen (1992, 2014) to calculate such relaxation transitions and average quantities has been used to illustrate the radiative and non-radiative spectra for aluminium and tungsten shown in Figure 1.5. Note that the spectra in Figure 1.5a,b shows all the possible transitions, but their importance from an energy point of view (probability × emission energy) can be better seen in Figure 1.5c,d, which shows the fraction of the element's binding energy (for a given shell) that corresponds to each single transition. It illustrates that non-radiative emissions (Auger electrons) are more important for low-Z elements, whereas for high-Z elements, the opposite occurs and radiative transitions (fluorescent x rays) are predominant.

The fluorescence yield ω_{S0} of a subshell is equal to the average number of x rays emitted in the filling of a vacancy in subshell S0 or, more generally, the fluorescence yield of a state with a vacancy in the subshell S0 is defined as the probability that the vacancy is filled through a radiative transition (cf. Llovet *et al.*, 2014)

$$\omega_{S0} = \sum_{S1} P_{S0-S1} \tag{1.35}$$

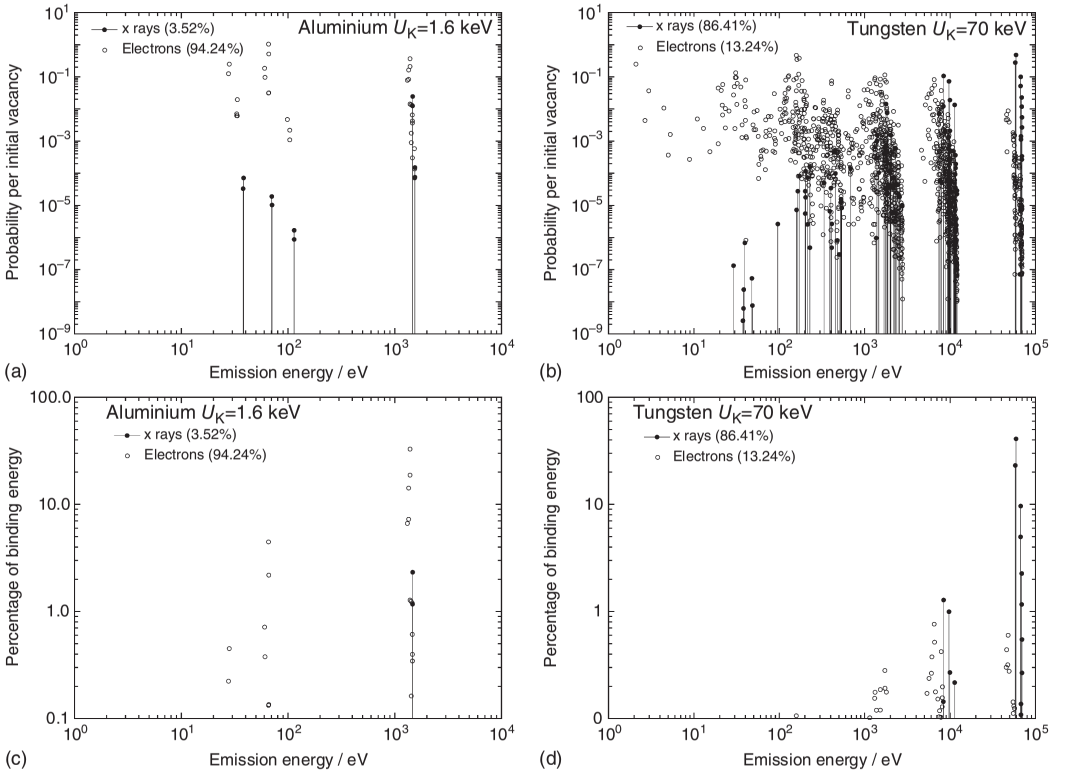

Figure 1.5 Radiative (filled circles and lines) and non-radiative (open circles) relaxation spectra from the K shell for aluminium ($Z = 13$, a and c) and tungsten ($Z = 74$, b and d). (a) and (c) show the probabilities of a given emission per initial vacancy, where the legends indicate the percentage of the element binding energy taken by all x rays and Auger electrons. (c) and (d) illustrate the percentage of U_K for each individual emission, showing that in low-Z elements most of the binding energy fraction corresponds to non-radiative emissions, whereas for high-Z elements, the highest fraction corresponds to radiative transitions. (Data calculated with the *RELAX* code, Cullen 1992, 2014).

The probability that a K x-ray will be emitted is close to unity in high-Z elements and nearly zero in low-Z elements. For a non-radiative transition, the Auger yield, a_{S0}, of a state with a vacancy in the S0 subshell is defined as

$$a_{S0} = \sum_{S1,S2} P_{S0-S1-S2} \tag{1.36}$$

and gives the average number of Auger electrons emitted through transitions that fill the original vacancy in S0. Evidently, from Eq. (1.34),

$$\omega_{S0} + a_{S0} = 1 \tag{1.37}$$

In the same way, the Coster–Kronig yield, $f_{S0,1}$, is the probability that a vacancy in the subshell S0 of a singly ionized atom shifts to a higher subshell S1 of the same shell ($n_1 = n_0$) through a non-radiative transition; that is,

$$f_{S0,1} = \sum_{S2} P_{S0-S1-S2} \tag{1.38}$$

where the sum is over subshells S2 above the active shell, with $n_2 > n_0$. A related quantity is the *intra-shell radiative yield*, $f'_{S0,1} = P_{S0-S1}$, which is equal to the probability that the vacancy moves from S0 to S1 ($n_1 > n_0$) through a radiative transition. The sum

$$\eta_{S0,S1} = f_{S0,1} + f'_{S0,1} = P_{S0-S1} + \sum_{S2} P_{S0-S1-S2} \tag{1.39}$$

is the total probability of intra-shell transitions that shift the vacancy from S0 to S1. For a vacancy in a subshell S0, the total probability of inter-shell transitions that transfer the vacancy to subshell S1 of an outer shell ($n_1 > n_0$) is

$$\eta_{S0,S1} = P_{S0-S1} + \sum_{S2} P_{S0-S1-S2} \tag{1.40}$$

and similar expansions can be written for the Super Coster–Kronig yield.

Detailed reviews and data on radiative and non-radiative yields, as well as on fluorescent, Auger, and Coster–Kronig transition probabilities, have been published by Bambynek *et al.* (1972) and Krause (1979). Hubbell *et al.* (1994) have given semi-empirical expressions fitting experimental data for x-ray fluorescence yields from the K-, L-, and M-shells for any element, which are widely used. The basic Z dependence is in the form of a power series,

$$\omega_i = \sum_n c_n Z^n \tag{1.41}$$

where the subscript i = K, L, M; numerical values of the coefficients are given in Table 1.3.[4] It should be noted that $a_i = 1 - \omega_i$. The expressions of Hubbell *et al.*, were extended by Perkins *et al.* (1991a) to predict the fluorescence yields for individual subshells of the K-, L-, M-, N-, and O-shells. Values of the fluorescence

4 Note that this expression supersedes a formula introduced by Burhop (1955) for the K-shell yield having the form

$$\left(\frac{\omega_K}{1-\omega_K}\right)^{1/4} = \sum_{i=0}^{3} C_i Z^i$$

Table 1.3 K-, L-, and M-shell fluorescence yields fitted polynomials of the form $\omega_i = \sum_{n=0} c_n Z^n$ as a function of atomic number Z.

Fluorescence yield	Range of Z	Fitting coefficient				
		c_0	c_1	c_2	c_3	c_4
ω_K	11–19	1.4340×10^{-1}	-2.5606×10^{-2}	1.3163×10^{-3}	—	—
	20–99	-7.6388×10^{-1}	5.4070×10^{-2}	-4.0544×10^{-4}	-1.4348×10^{-6}	1.8252×10^{-8}
ω_L	26–51	-9.2521×10^{-2}	8.7531×10^{-3}	-2.8087×10^{-4}	3.4823×10^{-6}	—
	52–92	4.2193	-2.3520×10^{-1}	4.7911×10^{-3}	-4.1549×10^{-5}	1.3564×10^{-7}
ω_M	71–92	-4.587×10^{-2}	1.208×10^{-4}	1.051×10^{-5}	—	—

Source: Hubbell *et al.* (1994, erratum in 2004). Reproduced with permission of American Institute of Physics.

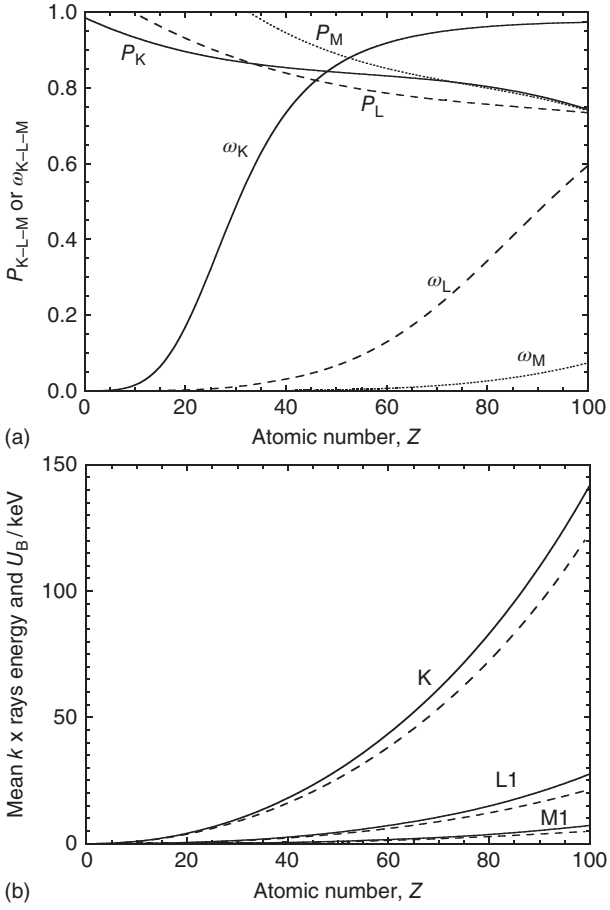

Figure 1.6 (a) Fluorescence yield, ω_i, and average fraction of fluorescent events (strictly, fractional participation in the photoelectric effect), P_i, by K-, L-, and M-shells; note that $a_i = 1 - \omega_i$. (b) Mean fluorescence x-ray energies, $\overline{k}_i$ (dashed lines), in the K-, L1-, and M1-shells; for comparison, the binding energies, $U_B(i)$ are also shown (solid lines).

yields, ω_i, and average fraction of fluorescent events, P_i, and fluorescence x-ray mean energies, $\overline{k}_i$, for different shells are given in Appendix A; they are illustrated in Figure 1.6.

---

where the coefficients have been re-fitted in reviews by different authors incorporating new sets of experimental data available (e.g., Bambynek *et al.*, 1972, 1984). Hubbell rewrote this expression as

$$\omega_K = \frac{\left[\sum_{i=0}^{3} C_i Z^i\right]^4}{1 + \left[\sum_{i=0}^{3} C_i Z^i\right]^4}$$

which has become widely used in the literature (e.g., Higgings *et al.*, 1992; Seltzer, 1993) and sometimes cited as developed by Hubbell himself (cf. Carron, 2007; McParland, 2010).

1.6.3 Emission Cross Sections

In practical calculations and in Monte Carlo simulations of radiation transport (see Chapter 8), cross sections for the emissions of characteristic x rays, σ_{S0-S1}, or Auger electrons, $\sigma_{S0-S1-S2}$, need to be considered for the different elements. They are obtained, by measurement or by calculation, from the number of x rays or Auger electrons emitted from a given transition.

The probability that an incident photon or electron gives rise to a characteristic x-ray emission or an Auger electron is $\sigma_{S0-S1}\ n_a\ t$ or $\sigma_{S0-S1-S2}\ n_a\ t$, where n_a is the number of atoms per unit volume and t is the thickness of a thin foil of the element. To calculate the emission cross sections σ_{S0-S1} and $\sigma_{S0-S1-S2}$, the cross section for the ionization of the subshell S0 is required for the energy of the incident particle, $\sigma_{S0}(E)$. Hence, for example, for x rays and Auger electrons generated from ionizations of the K-shell (S0 = K),

$$\sigma_{K-S1} = \sigma_K(E)\ P_{K-S1} \quad \text{and} \quad \sigma_{K-S1-S2} = \sigma_K(E)\ P_{K-S1-S2} \tag{1.42}$$

where P_{K-S1} and $P_{K-S1-S2}$ are the probabilities for the corresponding radiative and non-radiative transitions. The calculation is, however, quite complex for subshells other than the K-shell because account has to be made for vacancies in a subshell produced not only by the direct ionization by an incident particle but also during the de-excitation cascade of vacancies generated in other subshells; recall that during the de-excitation process of the atom, the initial vacancy migrates to outer subshells and in the case of non-radiative transitions, additional vacancies are generated. Unfortunately, information on the relaxation of multi-vacancy states is not generally available.

1.7 Evaluation of Uncertainties

Following a recommendation of the Comité International des Poids et Mesures (CIPM, 1981), the International Organization for Standardization (ISO) developed the *Guide to the Expression of Uncertainty in Measurement* (ISO, 1993), known as the GUM, for the evaluation of uncertainties based on a new unified approach. The current evaluation of measurement uncertainties worldwide is based on these procedures. In the United States, the NIST published Technical Note 1297 in 1994 summarizing the GUM recommendations (Taylor and Kuyatt, 1994). Minor corrections and a supplement have subsequently been published by the BIPM, developed by the Joint Committee for Guides in Metrology (JCGM, 2008a, 2008b). This section describes the practical implementation of the GUM recommendations, partly based on summaries published in IAEA TRS-398 (Andreo *et al.*, 2000) and in IAEA TRS-457 (Alm-Carlsson *et al.*, 2007) that are applicable to the measurements and calculations that will be described in subsequent chapters.

1.7.1 Accuracy and Precision – Error and Uncertainty

The GUM defines *accuracy* as the closeness of the agreement between a result and a true value. This definition is adopted from the *International Vocabulary*

of Basic and General Terms in Metrology (VIM) published by the ISO (1993). The GUM clarifies that in fortuitous circumstances a result can be very accurate (i.e., be close to the 'true' value, or have a negligible error) while at the same time having a large uncertainty. Accuracy (characterized by a single value) and uncertainty (characterized by a distribution) are two different concepts, but often they are used interchangeably, creating confusion. The same occurs with the term *precision*, which the GUM emphasizes should not be used for accuracy, as it describes the extent to which a given result can be repeated or reproduced; the terms *repeatability* and *reproducibility* are recommended.

The terms *error* and *uncertainty* have also traditionally been used interchangeably; however, the current approach makes a clear distinction between these two concepts.

(a) An error has traditionally been viewed as having two components: a *random* component and a *systematic* component. According to the current approach, an *error* is the difference between a measured value and the *true* value of the measurand. If errors were known exactly, the true value could be determined; in reality, errors are estimated in the best possible way and corrections are made for them. Therefore, after application of all known corrections, errors do not need any further consideration (their expectation value being zero) and the quantities of interest are uncertainties. An error has both a numerical value and a sign.

(b) The *uncertainty* associated with a measurement is a parameter that characterizes the dispersion of the values 'that could reasonably be attributed to the measurand'. This parameter is normally an estimated standard deviation. Such an uncertainty has no known sign and is usually assumed to be symmetric.[5] It is a measure of our lack of exact knowledge after all recognized *systematic* effects have been eliminated by applying appropriate corrections. The uncertainty of a measurement is expressed as a standard uncertainty relative to the mean value and the evaluation of standard uncertainties is classified into *Type A* and *Type B*. The method of evaluation of Type A standard uncertainties is by statistical analysis of a series of observations. The method of evaluation of Type B standard uncertainties is based on means other than statistical analysis of a series of observations. This is in contrast to the traditional categorization of uncertainties into random and systematic contributions.

In the past, uncertainties have often been evaluated in the form of confidence limits, usually at the 95% confidence level. This approach is no longer used because there is no statistical basis for combining confidence limits. The law of propagation of uncertainty requires a combination in terms of variances, as will be discussed in Section 1.7.5.

5 There are cases in which the dispersion is known to be asymmetric and for which a characterization other than a standard deviation is appropriate. It is also possible to have a measurement scenario in which the dispersion is one-sided, in which case the uncertainty does have a sign.

1.7.2 Type A Standard Uncertainty

Given a series of N measurements with values x_i, each with equal weight, the best estimate of the quantity x is given by the *arithmetic mean* value of the measured values

$$\bar{x} = \frac{1}{N}\sum_{i=1}^{N} x_i \tag{1.43}$$

The distribution of the N measured values x_i around their mean value $\bar{x}$ can be characterized by the *standard deviation of the sample*, given by

$$s(x_i) = \sqrt{\frac{1}{N-1}\sum_{i=1}^{N}(x_i - \bar{x})^2} \tag{1.44}$$

and the quantity $s^2(x_i)$ is the *sample variance*. We are often interested in the *standard deviation of the mean value*, written as $s(\bar{x})$, for which the general expression is

$$s(\bar{x}) = \frac{1}{\sqrt{N}}\, s(x_i) \tag{1.45}$$

which can, in principle, be reduced by increasing the number N of measurements.

A more general situation is the estimate of $s(\bar{x})$ for several groups of measurements, where statistical weights have to be used. Given N groups, each with a mean value $\bar{x}_i$ and standard deviation of the mean s_i, the *weighted mean value* and the *standard deviation of the weighted mean* are respectively given by

$$\bar{x}_w = \frac{\sum_{i=1}^{N} w_i\, x_i}{\sum_{i=1}^{N} w_i} \tag{1.46}$$

and

$$s(\bar{x}_w) = \frac{1}{\sqrt{\sum_{i=1}^{N} w_i}} \tag{1.47}$$

where $w_i = 1/s_i^2$.

Cases can be found where experimental or calculated values (e.g., determined by different groups or by different methods) show a larger or smaller dispersion than what could reasonably be predicted from the stated uncertainties. In these cases, the Birge test (Birge, 1932) can be used to assess the consistency of the data set. The test compares the so-called *internal* and *external* variances, where the former corresponds to the prediction based on Eq. (1.47) and the usual laws of propagation of uncertainty (see Section 1.7.5), while the latter describes the outcome in terms of fluctuations around the weighted mean value. The Birge ratio, R_{Birge}, is obtained from[6]

6 Interested readers might observe the similarity of the Birge ratio and the chi-squared per degree of freedom.

$$R^2_{\text{Birge}} = \frac{s^2_{\text{ext}}}{s^2_{\text{int}}} = \frac{\left[\dfrac{\sum_{i=1}^{N} w_i (x_i - \bar{x}_w)^2}{(N-1)\sum_{i=1}^{N} w_i}\right]}{\dfrac{1}{\sum_{i=1}^{N} w_i}} = \sum_{i=1}^{N} \frac{w_i (x_i - \bar{x}_w)^2}{N-1} \tag{1.48}$$

If R_{Birge} is significantly larger than unity, that is, the outcome is more scattered than the prediction, then it is likely that at least some of the variances s_i are underestimated, and the converse can also be inferred. The Birge test is used, for example, for some of the CODATA recommended values of fundamental physical constants (Mohr *et al.*, 2012). In some statistical treatments, modified weights are assigned to force the Birge ratio to be unity (see, e.g., Mandel and Paule, 1970; Andreo *et al.*, 2013). The need for such consistency tests illustrates the fact that uncertainties evaluated using the methods described are, by their nature, only estimates of the most probable deviation of each measured value from the true value.

The *standard uncertainty of Type A*, denoted by u_{A}, corresponds to the standard deviation of the mean value, that is

$$u_{\text{A}} = s(\bar{x}) \tag{1.49}$$

1.7.3 Type B Standard Uncertainty

There are many uncertainty sources that cannot be estimated by repeated measurements; they are called *Type B uncertainties*. These include not only the known effects of quantities such as pressure, temperature, application of correction factors, or physical data taken from the literature, but also the effects of unknown, although suspected, influences on the measurement process.

Type B uncertainties must be estimated so that they correspond to standard deviations, that is, they are *Type B standard uncertainties*, denoted by u_{B}. It is helpful to assume that these uncertainties have a probability distribution that corresponds to some shape for which the statistical treatment is known.

In this respect, it is sometimes assumed that Type B uncertainties can be described by a rectangular probability density, that is, that the true value has an equal probability of lying anywhere within the given maximum limits $-L$ and $+L$. With this assumption, it can be shown that the Type B standard uncertainty is given by

$$u_{\text{B}} = \frac{L}{\sqrt{3}} \tag{1.50}$$

Alternatively, if it is assumed that the distribution is triangular (with the same limits), the Type B standard uncertainty is given by

$$u_{\text{B}} = \frac{L}{\sqrt{6}} \tag{1.51}$$

Another treatment is to start with the assumption that Type B uncertainties have a distribution that is approximately Gaussian. The Type B standard uncertainty can in this case be derived by first estimating some limits $\pm L$ and then dividing

that limit by a suitable number. If, for example, the experimenter is *fairly sure* of the limit L, it can be considered to correspond approximately to a 95% confidence limit, whereas if the experimenter is *almost certain*, it may be taken to correspond approximately to a 99% confidence limit. Hence, the Type B standard uncertainty can be obtained from

$$u_B = \frac{L}{k} \tag{1.52}$$

where $k = 2$ if the experimenter is fairly sure and $k = 3$ if the experimenter is almost certain of the estimated limits $\pm L$. This relation corresponds to the properties of a Gaussian distribution and it is usually not worthwhile to apply divisors other than 2 or 3 because of the approximate nature of the estimation.

There are thus no rigid rules for estimating Type B standard uncertainties. The experimenter should use the best knowledge and experience and, whichever method is applied, provide estimates that can be used as if they were standard deviations. Because of the approximations involved, Type B uncertainties should not normally be stated with a resolution better than 10% or 20%.

1.7.4 Combined and Expanded Uncertainty

As emphasized above, estimated Type A and Type B uncertainties correspond to standard deviations and therefore they can be combined using the law of propagation of uncertainty combining variances (the squares of standard deviations). If u_A and u_B are, respectively, the Type A and Type B standard uncertainties of the value of a quantity, the *combined standard uncertainty* of that value is

$$u_c = \sqrt{u_A^2 + u_B^2} \tag{1.53}$$

which also has the character of a standard deviation. If, in addition, it is believed to have a Gaussian probability density, then the standard deviation corresponds to a confidence limit of about 67%.

It is sometimes desirable to multiply the combined standard uncertainty by a suitable factor, called the *coverage factor*, k, to yield an *expanded uncertainty*. Values of the coverage factor of $k = 2$ or 3, correspond typically to confidence limits of about 95% or 99%. In either case, the numerical value of the coverage factor should be clearly indicated. The result of a measurement will thus be expressed by

$$\overline{x} \pm k\, u_c \tag{1.54}$$

The approximate nature of uncertainty estimates, in particular for Type B, makes it doubtful that more than one significant figure is ever justified in choosing the coverage factor.

1.7.5 Law of Propagation of Uncertainty

A given measurand Y is usually not measured directly, but is determined from N other quantities X_i through a relation

$$Y = F(X_1, X_2, \ldots, X_N) \tag{1.55}$$

where X_i are different quantities, experimental methods, corrections, different time, or experimenters, etc. F should not be considered a function in the proper sense, but rather a description of the complete measurement process.

An *estimate* y of the measurand Y is obtained from estimates x_i (described by appropriate probability distributions) of the different quantities X_i, that is

$$y = f(x_1, x_2, \ldots, x_N) \tag{1.56}$$

The estimated combined standard uncertainty of the measurement, $u_c(y)$, including all estimates x_i and their uncertainties $u(x_i)$, can be obtained from (see, e.g., the GUM)

$$u_c^2(y) = \sum_{i=1}^{N} \left(\frac{\partial f}{\partial x_i} \right)^2 u^2(x_i) + 2 \sum_{i=1}^{N} \sum_{j=i+1}^{N} \frac{\partial f}{\partial x_i} \frac{\partial f}{\partial x_j} u(x_i, x_j) \tag{1.57}$$

where $u(x_i, x_j)$ is the estimated *covariance* associated with x_i and x_j; note that $u(x_i, x_j) = u(x_j, x_i)$. The degree of correlation between x_i and x_j is given by the *correlation coefficient*

$$r(x_i, x_j) = \frac{u(x_i, x_j)}{u(x_i)\, u(x_j)} \tag{1.58}$$

If we make the transformation $u_i(y) \equiv |\partial f / \partial x_i|\, u(x_i)$, Eq. (1.57) becomes

$$u_c^2(y) = \sum_{i=1}^{N} u_i^2(y) + 2 \sum_{i=1}^{N} \sum_{j=i+1}^{N} u_i(y)\, u_j(y)\, u(x_i, x_j) \tag{1.59}$$

that corresponds to the estimated combined variance of the measurement when the input quantities x_i are *correlated*. For independent or *uncorrelated* quantities, the second term in Eq. (1.59) cancels out, as $u(x_i, x_j) = 0$, and the estimated combined variance takes the form

$$u_c^2(y) = \sum_{i=1}^{N} u_i^2(y) \tag{1.60}$$

that is, the estimated combined standard uncertainty is obtained as the square root of the variance.

Expressions (1.59) and (1.60) constitute what is termed by the GUM and others as the *Law of propagation of uncertainty*. This is often referred to in the literature as 'the law of error propagation' but, as emphasized earlier, in the current nomenclature the term 'error' is used for a different purpose.

To conclude the section on uncertainties, it should be emphasized that the old terms 'random' and 'systematic' uncertainties *do not* have a one-to-one correspondence to Type A and Type B uncertainties. Readers should also be warned that in spite of the remarks made throughout this section, available in the cited GUM references for many years now, the scientific literature still uses, sometimes incorrectly, terms such as precision and accuracy, classifies uncertainties by their nature (random and systematic) rather than by their method of determination (Type A and Type B), considers errors as uncertainties or combines the two, or

uses the absolute difference between values as an estimate of the uncertainty. Caution is therefore advised in the reading of references.

Exercises

1 What is the photon energy range corresponding to the UV radiation band?
Answer: 10 nm–400 nm corresponds to 124 eV–3.1 eV.

2 For a kinetic energy of 100 MeV, calculate the velocity, β, for (a) electrons, (b) protons, and (c) α particles. The corresponding rest energies are given in Appendix A.
Answer: (a) 0.9999; (b) 0.4282; (c) 0.2271.

3 Conversely, given a value of $\beta = 0.95$, calculate the corresponding kinetic energies of electrons, protons and α particles
Answer: (a) 1.1255 MeV; (b) 2066.6 MeV; (c) 8209.86 MeV.

4 The result of a given process is derived as the product of several independent quantities, $Q = \prod q_i$. The Type A and Type B uncertainty of each q_i, $(u_A, u_B)_i$, given as a relative standard uncertainty, are (0.1, 0.5), (0.01, 0.1), (0.02, 0.4), and (0.3, 0.19). Determine the combined standard uncertainty of Q.
Answer: $u_c(Q) = 0.75$.

5 Given the following set of data (75.4, 79.7, 75.0, 77.0, 78.4), with standard uncertainties (0.95, 0.5, 0.2, 1.2, 0.8), determine the non-weighted and weighted means and the corresponding Type A uncertainties. Determine the Birge ratio for the data and comment on the uncertainty estimates of the data.
Answer: $\overline{x} = 77.1$, $s(\overline{x}) = 0.89$; $\overline{x}_w = 75.8$, $s(\overline{x}_w) = 0.18$; $R_{Birge} = 2.2$.

6 Using the half-width of the set of data in the previous exercise, estimate the Type B uncertainty assuming rectangular, triangular, and Gaussian (with $k = 2$) distributions. Which of the three is considered to be more conservative?
Answer: $u_{B\,rect} = 1.36$, $u_{B\,trian} = 0.96$, $u_{B\,Gauss} = 1.18$.
The rectangular distribution is a special case, because in general for most data sets there is a higher probability that the true value lies nearer to the middle than at the extremes. This leaves the triangular and Gaussian ($k = 2 \rightarrow 95\%$) distributions as conceptually similar, with the 95% Gaussian being more conservative.